Songklanakarin J. Sci. Technol.
44 (3), 728–734, May – Jun. 2022

http://www.sjst.psu.ac.th

Original Article

Novel environmentally friendly catalytic oxidation approaches on elemental mercury removal from carbon steel surface

Ihsan Wan Azelee[1], Azmi Aris[1*], and Wan Azelee Wan Abu Bakar[2]

[1] *Centre for Environmental Sustainability and Water Security (IPASA), Universiti Teknologi Malaysia, Skudai, Johor, 81310 Malaysia*

[2] *Department of Chemistry, Faculty of Science, Universiti Teknologi Malaysia, Skudai, Johor, 81310 Malaysia*

Received: 25 July 2021; Revised: 5 December 2021; Accepted: 18 December 2021

Abstract

To date, technology for the removal of elementary mercury adsorbed on carbon steel surfaces with very minimum iron (Fe) leaching is apparently missing. In this study, the oxidation reaction of mono-peroxyacetic acid (PAA) was used in the presence of $Ru/Mn/Al_2O_3$ catalyst to enhance the treatment removal. The obtained results revealed that the PAA alone could reduce 91% of Hg° removal in 3 h. Interestingly, with the presence of $Ru/Mn/Al_2O_3$ catalyst calcined at 1000°C, the PAA managed to remove almost 99% of Hg° at the same treatment time with the lowest Fe leaching of 17 ppm.

Keywords: mercury, carbon steel, catalyst, peroxyacetic acid, Fe leaching

1. Introduction

It is well established that mercury is capable to seriously impact human health, living creatures as well as the environment. Hg° is difficult to remove because of its insolubility and volatility (Zhang *et al.*, 2020). Unlike Hg°, oxidized mercury (Hg^{2+}) and particulate bound mercury (Hg^p) can be easily removed through dissolution in wet flue gas desulfurization and by dust-removal devices (Zhao *et al.*, 2019). Thus, many technologies have been studied to remove mercury from aqueous, solid waste, or gas streams (Chalkidis, Jampaiah, Hartley, Sabri, & Bhargava, 2020). However, there are very limited reports available on the removal of Hg° from the metal surface (Chaiyasit, Kositanont, Yeh, Gallup, & Young, 2010; Ebadian, 2001). Carbon steel is commercially available utilized in the manufacturing of reaction vessels and is a common constructional material for many industrial units because of its low cost and excellent mechanical properties. However, amalgam corrosion due to Hg° contamination on carbon steel may lead to brittle fracture, causing significant economic losses and environmental pollution (Cai, He, Zeng, Wang, & Huang, 2018; Nengkoda *et al.*, 2009).

The utilization of acid to treat mercury spills and surface pollution is disfavored due to the wellbeing risks to laborers and the erosion of steel surfaces present on most downhole instruments (Chalkidis *et al.*, 2020; Jafari, Akbarzade, & Danaee, 2019). One of the innovations being reported includes mobilizing mercury utilizing a lixiviant of potassium iodide/iodine aqueous solution (Chaiyasit *et al.*, 2010; Ebadian, 2001; Foust, 1993; Mattigod, Feng, Fryxell, Liu, & Gong, 1999). This patented process utilizes the oxidation and complex formation reactions for the high efficiency of mercury removal (Mattigod *et al.*, 1999). However, further study needs to be conducted to encounter several disadvantages such as longer treatment time, additional steps for waste disposal required, and the Fe leaching of the carbon steel (Chaiyasit *et al.*, 2010). These shortages contrarily facilitate the fast development of oxidation technology. Numerous applied researches on PAA have been reported in different fields (Kerkaert *et al.*, 2011; Qu, Jiang, Li, Bai, & Zhou, 2008; Rohtash, Singh, & Kumar, 2014; Zhao, Hao, & Guo, 2014). Due to the strong oxidation

*Corresponding author
Email address: azmi.aris@utm.my

capability of PAA, the potential of its application on mercury removal was further studied.

Upon application, the catalyst was found to be a co-benefit for mercury removal (Hao *et al.*, 2020; Zhang *et al.*, 2020; Zhao *et al.*, 2019; Zhuang, Laumb, Liggett, Holmes, & Pavlish, 2007). The importance of solid base catalysts is recognized for their eco-friendly qualities. Metal oxides are identified as the most used catalysts. Aluminum oxide (Al_2O_3) has been generally employed as a support material due to its beneficial effects such as high surface area, developed pore structure, and well-characterized acid-base properties of the surface (Garbarino, Riani, Magistri, & Busca, 2014). Rosid, Toemen, Wan Abu Bakar, Zamani, and Wan Mokhtar (2019) observed that the incorporation of ruthenium into manganese oxide catalyst showed a positive effect on methanation reaction. This is similar to the finding of Panagiotopoulou, Kondarides, & Verykios (2009), where CO_2 methanation was strongly favored with the increase in Ru content.

This study examined the application of PAA assisted by the $Ru/Mn/Al_2O_3$ catalyst for Hg° removal with minimum Fe leaching from the carbon steel surface. Factors impacting Hg° removal, Fe leaching, and treatment time were investigated. From our review, previous studies have only emphasized Hg° removal from its supporting materials, and no study has been reported to determine the Fe leaching from carbon steel surface during the removal process. This aspect of the study is very crucial as the Fe leaching occurrence will affect the mechanical properties of the carbon steel leading to cracking and brittleness of the surface material (Jafari *et al.*, 2019; Siddiqui, Abdul-Wahab, Pervez, & Qamar, 2007).

2. Materials and Methods

2.1 Materials

Hydrogen peroxide (H_2O_2 30%, Merck) and glacial acetic acid (GAA, Merck) were used in PAA preparation. Iodine (I_2) and potassium iodide (KI) were purchased from Sigma and Merck respectively and were used for the preparation of I_2/KI lixiviant. Liquid Hg° was supplied by Merck. Ruthenium (III) chloride hydrate ($RuCl_3.H_2O$, Merck), Manganese (II) chloride dehydrate ($MnCl_2.2H_2O$, Merck), Aluminum oxide beds (Al_2O_3, 3 mm, Sigma Aldrich), and $AgNO_3$ reagent were used in catalyst preparation. All chemicals were used as received without further purification. The SAE J429 carbon steel was purchased from a local hardware shop.

2.2 Preparatory work

2.2.1 Mercury adsorption

SAE J429 carbon steel was applied and contaminated with Hg° using a physisorbed method for mercury adsorption to occur (Chaiyasit *et al.*, 2010). During the preparation, the carbon steel was immersed directly into 0.3 kg of liquid Hg° and left for 30 d for the physisorption of liquid Hg° on the carbon steel surface to occur.

2.2.2 Preparation of PAA

PAA was prepared from H_2O_2 and GAA. In this study, 1000 ppm PAA with mole ratio H_2O_2 to GAA 1:1 was applied for Hg° removal. During the preparation, 1.24 ml of H_2O_2 and 0.75 ml of GAA were mixed, stirred, and diluted with deionized water in a volumetric flask (1 L).

2.2.3 Preparation of I2/KI lixiviant

The lixiviant solution was prepared by mixing I_2 and KI chemical powder with concentrations of 0.1M and 0.5M, respectively. During the preparation of the I_2/KI solution, 12.69 g of I_2 and 41.5 g of KI were weighted and diluted with deionized water in a volumetric flask (500 mL). The prepared I_2/KI lixiviant was stored in a glass bottle covered with aluminum foil until used.

2.2.4 Preparation of catalyst

The aqueous incipient wetness impregnation method was used to synthesize $Ru/Mn/Al_2O_3$ catalysts (Rosid *et al.*, 2019; Toemen, Abu Bakar, & Ali, 2016). The amount of 1.03 g $RuCl_3.H_2O$ (dopant) and 5 g $MnCl_2.2H_2O$ (base) based on the molecular mass ratio of Ru and Mn at 25:75 was dissolved in 5 mL of distilled water at room temperature. This was followed by the impregnation with 5 g of Al_2O_3 beads (supported catalyst) for 15 min. They were then dried at ambient temperature. The impregnation and drying were repeated thrice. The beads were then washed with triply refined water to remove chloride ions until no change occurred when the $AgNO_3$ reagent was added. It was then aged at 80 °C for 24 h and calcined in an oxygen atmosphere at 400°C for 12 h. The potential catalyst was further calcined at various calcination temperatures of 400°C, 700°C, 900°C, 1000°C, and 1100°C; each of this was carried out for 5 h using a ramp rate of 10°C/min to remove all the metal counterions and water present in the catalyst.

2.3 Analytical method and characterization

Samples were collected from the solutions before the treatment reaction (as blank) and after the treatment reaction. The amount of oxidized Hg° present in the solution was examined using a mercury-hydride atomic absorption spectrometer (MHS-AAS) while Flame-ASS, Perkin Elmer AA400 was used to determine the amount of Fe due to leaching of carbon steel during treatment. In this study, Fe leaching was used to represent carbon steel as the majority of its composition (99 %) contained Fe while the rest are carbon, manganese, silica, phosphorus, sulfur chromium, and nickel (Jafarzadegan, Feng, Abdollah-zadeh, Saeid, Shen, & Assadi, 2012). The Fe leaching from carbon steel surface was determined by the amount of leached Fe found in the aqueous solution.

The prepared catalyst was characterized using X-ray Diffraction (XRD, Bruker AXS D8 Automatic Powder Diffractometer), Field Emission Scanning Electron Microscopy and Energy Dispersive X-Ray (FESEM-EDX, JEOL JSM-6701F), and Nitrogen Absorption (NA, Quantachrome Autosorb-1).

2.4 Hg° removal treatment

During Hg° removal treatment, the contaminated carbon steel was fully immersed with the PAA in a sealed bottle sample (250 mL) for 5 h. The PAA treatment conditions were applied at room temperature without stirring. Different treatment conditions of PAA, which include left soaking with no stirring at room temperature (Not Stir), stirring at room temperature (Stir), and stirring at 35–40°C (Stir + Heat) were applied. During the addition of Ru/Mn/Al_2O_3 catalyst, 0.6 % of the calcined catalyst at 400°C, 700°C, 9000C, 1000°, and 1100°C were added into the PAA solution separately during the treatment process. The performance of PAA was also compared with I_2/KI lixiviant without and with catalyst calcined at 1000°C. In this comparison study, the I_2/KI lixiviant was stirred at 35-40°C which showed a higher performance of Hg° removal (the results were not included). At least three replicates were done for each experiment. After the reaction ended, the treatment solution was collected for Hg° removal and Fe leaching analysis. The initial treatment solution without Hg° contaminated carbon steel was used as a blank. The carbon steel sample was removed and rinsed with distilled water for subsequent testing.

3. Results and Discussion

3.1 Removal of Hg° and Fe leaching

The experiments of Hg° removal were carried out stepwise by (i) comparing PAA with I_2/KI lixiviant in the absence or the presence of Ru/Mn/Al_2O_3 catalyst, (ii) varying treatment condition of PAA, and (iii) varying calcination temperature of Ru/Mn/Al_2O_3 catalyst.

Based on Figure 1, both the PAA and I_2/KI lixiviant were capable of removing Hg° from carbon steel by above 90%. However, the use of PAA took a shorter treatment time of 3 h as it obtained a chemical equilibrium at 91% of Hg° removal as shown by a constant percentage removal of Hg° compared to the I_2/KI lixiviant which took 14 h of treatment time with 94% of Hg° removal. The advantage of PAA was in agreement that the surface oxygen complexes of the carbonyl groups gave possible active sites for chemisorption and oxidation of Hg° (Tong *et al.*, 2017; Wigfield & Perkins, 1985). As for the I_2/ KI lixiviant, based on Khaing, Sugai, and Sasaki (2019) who studied the aspects of gold leaching using iodide-iodine solutions, it was determined that the oxidation for Hg° removal occurred after the production of triiodide (I^{3-}) between I_2 and KI in I_2/ KI lixiviant. Hence, I_2/KI lixiviant took a longer treatment time, thereby exhibited high Fe leaching of carbon steel at 360 ppm compared to PAA at 21 ppm (Chaiyasit *et al.*, 2010).

From the overall observation, the addition of the Ru/Mn/Al_2O_3 catalyst calcined at 1000°C successfully enhanced the removal treatment of Hg° for both PAA and I_2/ KI lixiviant. This involved the increase of Hg° percentage removal for both PAA (91% to 99%) and I_2/KI lixiviant (from 94% to 99%) and reduced the amount of Fe leaching for both PAA (21 ppm to 17 ppm) and lixiviant (from 360 ppm to 17.5 ppm). In the case of the treatment time, PAA successfully achieved the optimum removal at 3 h, compared to I_2/KI lixiviant, from 14 h to 6 h.

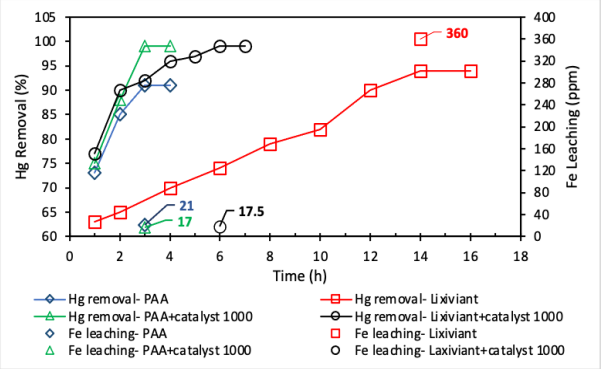

Figure 1. The removal of Hg° and the amount of Fe leaching from carbon steel in the presence of Ru/Mn/Al_2O_3 catalyst calcined at 1000°C over lixiviant and PAA treatment

The profile of Hg° removal at different experimental conditions of PAA is shown in Figure 2. It shows that the Hg° removal process for PAA continued to increase until 3 h and achieved chemical equilibrium after 3 h of reaction time, giving the highest percentage of Hg° removal at 99% when the treatment condition involved only soaking at room temperature (no stirring). When stirring or/and heating (Stir and Stir & Heat) were applied during the treatment, the reactions reached earlier chemical equilibrium at 2 h but achieved slightly lower Hg° removal of 96% and 97%, respectively. According to Qu *et al.* (2008), PAA is a high-energy state compound and as such can be considered thermodynamically unstable; so, there is a strong tendency for PAA to decompose into acetic acid and peroxide when the solution is heated. When this happens, PAA loses its oxidation power to remove Hg°.

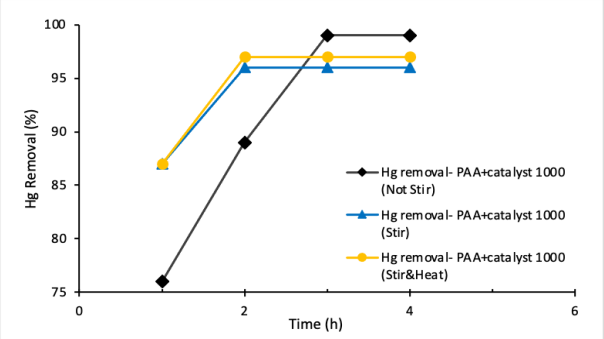

Figure 2. The percentage removal of Hg° from carbon steel by the addition of Ru/Mn/Al_2O_3 catalyst calcined at 1000°C over PAA at different treatment conditions (e.g., No Stir; Stir; Stir & Heat)

In the presence of Ru/Mn/Al_2O_3 catalyst (Figure 1), PAA exhibits three main advantageous criteria compared to I_2/KI lixiviant which are shorter treatment time, higher removal of Hg°, and a lower amount of Fe leaching. Therefore, the effect of the calcination temperature at 400°C, 700°C, 900°C, 1000°C, and 1100°C was studied on the Ru/Mn/Al_2O_3 catalyst as shown in Figure 3. The calcination temperature at 1000°C of the Ru/Mn/Al_2O_3 catalyst was

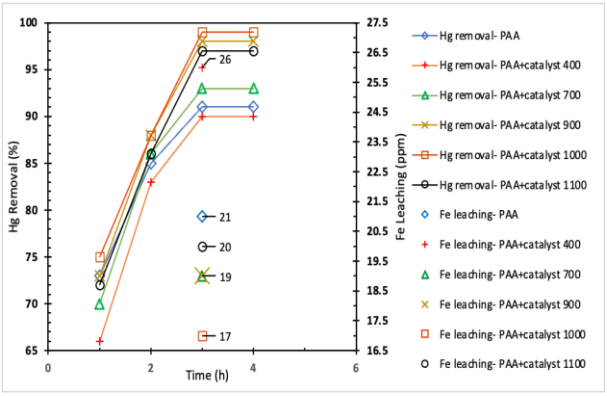

Figure 3. The percentage removal of Hg° using PAA in the presence of Ru/Mn/Al_2O_3 catalyst calcined at 400°C, 700°C, 900°C, 1000°C, and 1100°C for 4 h.

observed to yield the highest percentage removal of Hg° at 99% while at 400°C, 700°C, 900°C, and 1100°C yielded the removal of Hg° at 90.11 %, 92.75 %, 98.76 %, and 97.53 %, respectively. The calcination temperature of the catalyst at 400°C and 700°C were observed to have lower Hg° removal at not more than 93%. The Hg° removal increased when the calcination temperature increased from 900°C to 1000°C but decreased when the calcination temperature was further increased to 1100°C.

Figure 3 also shows the quantity of Fe leaching at the end of the Hg° removal study. The PAA with the calcined catalyst at 1000 °C showed the most effective Hg° removal as it provided the lowest amount of Fe leaching at 17 ppm. On the other hand, PAA with the calcined catalyst at 400 °C was less effective as it produced the highest Fe leaching at 26 ppm compared to the others studied at the calcination temperature. Meanwhile, the calcination temperature at 1100°C gave slightly higher Fe leaching at 20 ppm compared to 19 ppm at both 700°C and 900°C. Hence, Ru/Mn/Al_2O_3 catalyst calcined at 900°C, 1000°C, and 1100°C was characterized to seek an explanation for its effectiveness.

3.2 Characterization of catalysts

The characterization of Ru/Mn/Al_2O_3 catalysts calcined at temperature 900°C, 1000°C, and 1100°C was carried out by NA, XRD, FESEM, and EDX analyses.

3.2.1 Nitrogen adsorption analysis

Table 1 shows the surface area and pore diameter of the Ru/Mn/Al_2O_3 catalyst. The outcomes in terms of largest surface area and pore diameter are according to the order of 1000°C > 1100°C > 900°C of calcination temperature. At 1000°C, both surface area and pore diameter are the highest value at 9.576 m^2g^{-1} and 84.887 nm, respectively. A greater pore size generally generates a greater surface area of the catalyst, causing the availability of more active sites. Nevertheless, a higher calcination temperature at 1100°C prompts the sintering impact and causes the relocation of particle size to the grain which diminishes the surface area. Low calcination temperature of 900°C, however, are not able to increase the catalyst pore size, resulting in the low surface

Table 1. BET surface area (SBET) and BJH desorption average pore diameter, d(nm) of Ru/Mn/Al_2O catalysts calcined at 900˚C, 1000˚C, and 1100˚C for 5 h

Catalyst	Calcination temperature (°C)	S_{BET} (m^2g^{-1})	d (nm)
Ru/Mn-Al_2O_3	900	7.369	64.160
	1000	9.576	84.887
	1100	8.454	67.933

area. Based on this observation, the high catalytic activity accomplished at 1000°C calcination temperature was due to the higher surface area with greater pore size.

3.2.2 XRD Analysis

The potential catalyst of Ru/Mn/Al_2O_3 at 1000°C was further analyzed by XRD to determine the crystallinity and the actives species which contributed to the enhancement of the catalytic activity compared between calcination temperatures of 900°C and 1100°C. Figure 4 shows the diffractograms of the XRD pattern of Ru/Mn/Al_2O_3 catalysts. It could be recognized that the rhombohedral Al_2O_3 species was the alumina phase for active species besides the presence of active site species in hexagonal Mn_2O_3 and tetragonal RuO_2 phases. High crystallinity was shown to promote the existence of the active species as proven by the presence of those species when calcination temperature was increased from 900°C to 1000°C. Moreover, the peaks observed for Ru/Mn/Al_2O_3 catalyst become more intense, sharper, and narrower when increasing calcination temperature at 1000°C and 1100°C as also indicated by additional peaks of Al_2O_3 rhombohedral species at 2θ values of 76.869˚ and 76.901˚, respectively. Increasing calcination temperature led to good dispersion of active species on the catalyst surface. Rosid *et al.* (2019) also had observed an increase of active species in Ru/Mn/Nd/Al_2O_3 catalyst when calcination temperature increased from 900°C to 1000°C. However, the promotion of peak intensity of RuO_2 tetragonal at 1100°C may also decrease the surface area as shown by NA analysis. Hence, the presence of both the crystalline phase and high surface area provides the high catalytic activity of Ru/Mn/Al_2O_3 catalyst at 1000°C calcination temperature.

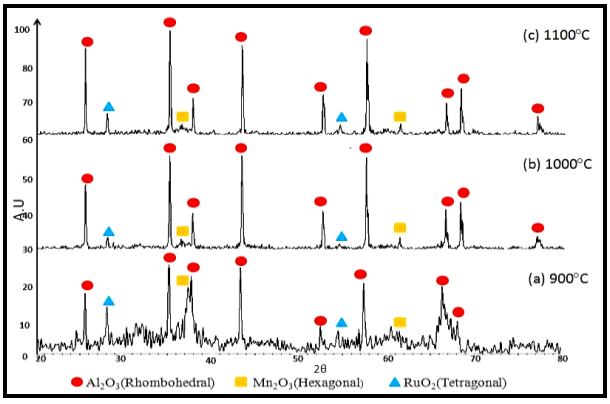

Figure 4. XRD Diffractograms of Ru/Mn/Al_2O_3 catalysts calcined at (a) 900°C (b) 1000°C (b) and (c) 1100°C for 5 h.

3.2.3 FESEM analysis

The morphology of $Ru/Mn/Al_2O_3$ catalyst calcined at 900°C, 1000°C, and 1100°C for 5 h are shown using FESEM micrographs in Figure 5. The catalyst calcined at 900°C shows that the particles were compact and aggregated with an undefined shape ranging from 98.8 nm to 688.8 nm. These particles' size is bigger compared to when it was calcined at 1000°C which varies from 41.4 nm to 85.1 nm. At 1000°C, the particles exhibit a cylindrical-like shape and are more defined on the catalyst surface. The particles were likewise appeared to extend out from the catalyst surface with high conglomeration. However, the particles with diameter sizes varying from 34.4 nm to 103.6 nm were shown to present at 1100°C with more agglomeration which corresponding to lower surface area as in aligned with the NA analysis result (Table 1).

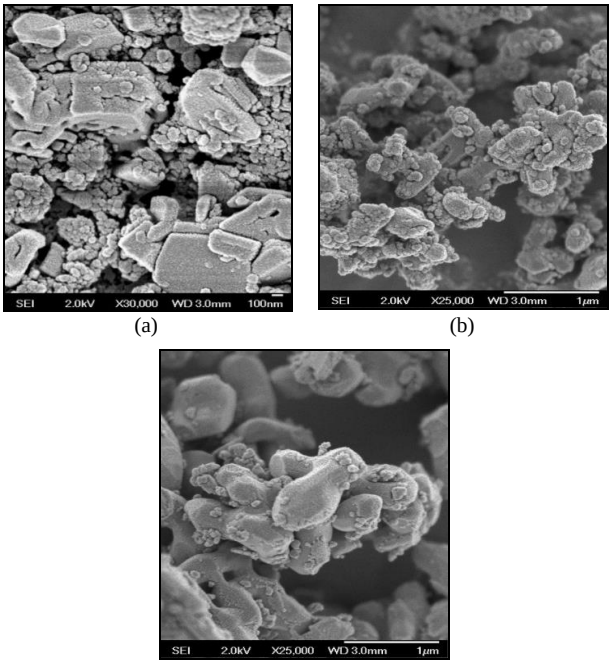

(a) (b) (c)

Figure 5. FESEM micrographs for fresh $Ru/Mn/Al_2O_3$ catalyst calcined at a) 900°C with magnification x30K, b) 1000°C with x25K, and c) 1100°C with magnification x25K for 5 h.

3.2.4 EDX analysis

Table 2 tabulates the elemental composition of the $Ru/Mn/Al_2O_3$ catalyst which was determined by FESEM-EDX. It was observed that Al, O, Mn, and Ru elements were present at all calcination temperatures. The presence of Al_2O_3 as dictated by the XRD examination was attributed to the presence of Al and O elements while both Mn and Ru elements presented as individual phases of MnO_2O_3 and RuO_2, respectively. The highest weight percentage of Al and O exhibits the dominant species of Al_2O_3 as the catalyst support. However, the higher of Mn at 900°C did not influence the catalytic activity as it acts just as a base for Ru active species on the Al_2O_3 support. Meantime, the high percentage of Ru at 1000°C supported the high Ru aggregation formation as indicates in the FESEM mapping profile. Thus, high synergist action at 1000°C calcination temperature was basically because of the existence of more Ru dynamic species.

Table 2. EDX analysis of $Ru/Mn/Al_2O_3$ catalyst calcined at 900°C, 1000oC, and 1100°C for 5 h.

Catalyst	Calcination temperature (°C)	Weight Ratio (%)			
		Al	O	Mn	Ru
$Ru/Mn/Al_2O_3$	900	42.53	25.43	8.80	2.85
	1000	39.69	31.59	7.47	3.41
	1100	42.33	30.05	6.05	1.20

3.3 Proposed mechanisms of the catalytic activity

Based on the removal study, we propose a possible mechanism for the catalytic activity reaction of $Ru/Mn/Al_2O_3$ catalyst on PAA for Hg° removal as shown in Figure 6. At the beginning of the reaction, PAA will react with $Ru/Mn/Al_2O_3$ catalyst (see No. 1) where the peroxide group (-O-O-) is unbounded (see No. 2). The reaction is expected to proceed with the dissociation of peroxyl radicals (ROO^-) and hydroxyl radicals (OH^-) (see No.3) (Kerkaert *et al.*, 2011). In the Hg° removal process (see No.4), ROO- radicals will react with Hg° to form mercury (I) acetate while OH^- radicals will form water as a side product. From our results, a plausible product of mercury (I) acetate (see No.5) can be assigned, observed as a white precipitate, soluble in HNO_3 and H_2SO_4, and insoluble in glacial acetic acid. Further confirmation was achieved when it yielded a grayish precipitate of mercury (I) oxide (Hg_2O_2) when the product of mercury (I) acetate reacted with KOH (Figure 7). The release of gases from the reaction also produced a 'pop' sound when it was tested with a lighted wooden splinter which suggested the existence of H_2 gas. The white precipitate mercury (I) acetate that was obtained at the end of the treatment could be easily filtered out for disposal.

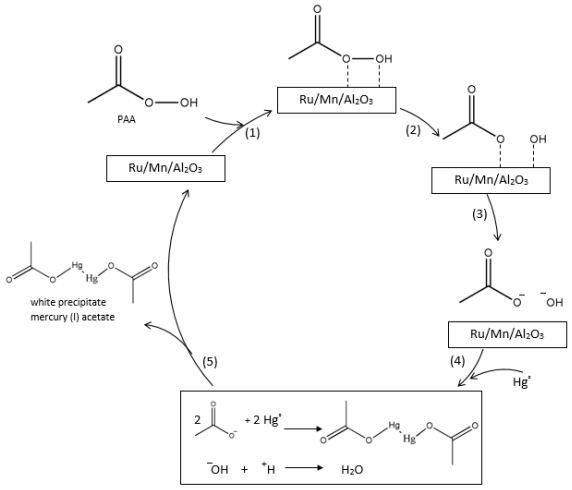

Figure 6. Proposed mechanism of the reaction between PAA and Hg° catalyzed by $Ru/Mn/Al_2O_3$ catalyst

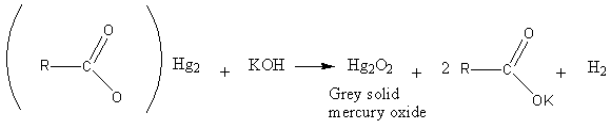

Figure 7. Confirmation test for mercury (I) acetate

This technique was more practical compared to the use of the lixiviant for Hg° removal. For the lixiviant, the complexed Hg° formed at the end process was soluble in the treated solutions and required further treatment for waste disposal. As reported by Mattigod *et al.* (1999), an effective adsorbent material consisting of self-assembled mercaptan groups on mesoporous silica (SAMMS) substrate is required to remove strongly complexed mercury from spent KI lixiviant. While the use of PAA will produce the stable insoluble solid of white precipitate mercury (I) acetate (the boiling point at 117°C) which can be easily separated from the waste without additional treatment. The catalyst will then proceed with its catalytic activity by adsorbing new PAA compounds on its surface. Thus, a cyclic catalytic reaction proceeds again.

4. Conclusions

The use of PAA in the presence of $Ru/Mn/Al_2O_3$ (calcined at 1000°C) achieved 99% Hg° removal in 3 h with the lowest amount of Fe leaching of 17 ppm from carbon steel surface at ambient temperature without stirring. The characteristics of the potential catalyst exhibited highest surface area (9.576 m2·g−1), highest average pore diameter (84.887 nm), high crystallinity phase with active species (RuO_2 with tetragonal phase, Mn_2O_3 with hexagonal phase, and Al_2O_3 support with rhombohedral phase), and possess high aggregation of nanoparticles size (41.4 to 85.1 nm). The obtained results prove that PAA in the presence of $Ru/Mn/Al_2O_3$ (calcined at 1000°C) catalyst offers a potential technology for the removal treatment of Hg° from the contaminated carbon steel surface.

Acknowledgements

This work was supported by the Ministry of Science, Technology, and Innovation, Malaysia (Vot. 78538); and Universiti Teknologi Malaysia (Vot. 04E87). We would also like to extend our deepest gratitude to Farah Ilyana Khaıruddın for her assistance during the experimental work.

References

Cai, Y., He, L., Zeng, J., Wang, X., & Huang, Y. (2018). The corrosion inhibition of imidazoline on the surface of X65 carbon steel in oxygen environment. *IOP Conference Series: Materials Science and Engineering*, *392*, 022018.

Chaiyasit, N., Kositanont, C., Yeh, S., Gallup, D., & Young, L. (2010). Decontamination of mercury contaminated steel of API 5L-X52 using iodine and iodide lixiviant. *Modern Applied Science*, *4*(1), 12–20.

Chalkidis, A., Jampaiah, D., Hartley, P. G., Sabri, Y. M., & Bhargava, S. K. (2020). Mercury in natural gas streams: A review of materials and processes for abatement and remediation. *Journal of Hazardous Materials*, *382*(August 2019), 121036.

Ebadian, M. A. (2001). *Mercury contaminated material decontamination methods: Investigation and assessment*. Miami, FL: Hemispheric Center for Environmental Technology.

Foust, D. F. (1993). *Extraction of mercury and mercury compounds from contaminated material and solutions*.

Garbarino, G., Riani, P., Magistri, L., & Busca, G. (2014). A study of the methanation of carbon dioxide on Ni/Al2O3 catalysts at atmospheric pressure. *International Journal of Hydrogen Energy*, *39*(22), 11557–11565.

Hao, R., Li, C., Wang, Z., Gong, Y., Yuan, B., Zhao, Y., Wang, L., & Crittenden, J. (2020). Removal of gaseous elemental mercury using thermally catalytic chlorite- persulfate complex. *Chemical Engineering Journal*, *391*, 123508.

Jafari, H., Akbarzade, K., & Danaee, I. (2019). Corrosion inhibition of carbon steel immersed in a 1 M HCl solution using benzothiazole derivatives. *Arabian Journal of Chemistry*, *12*(7), 1387–1394.

Jafarzadegan, M., Feng, A., Abdollah-zadeh, A., Saeid, T., Shen, J., & Assadi, H. (2012). Microstructural characterization in dissimilar friction stir welding between 304 stainless steel and st37 steel. *Materials Characterization*, *74*, 28–41.

Kerkaert, B., Mestdagh, F., Cucu, T., Aedo, P. R., Ling, S. Y., & Meulenaer, B. De. (2011). Hypochlorous and peracetic acid induced oxidation of dairy proteins. *Journal of Agricultural and Food Chemistry*, *59*, 907–914.

Khaing, S. Y., Sugai, Y., & Sasaki, K. (2019). Gold dissolution from ore with iodide-oxidising bacteria. *Scientific Reports*, *9*, 4178.

Mattigod, S. V., Feng, X., Fryxell, G. E., Liu, J., & Gong, M. (1999). Separation of complexed mercury from aqueous wastes using self-assembled mercaptan on mesoporous silica. *Separation Science and Technology*, *34*(12), 2329–2345.

Nengkoda, A., Reerink, H., Hinai, Z., PDO, Supranto, Prasetyo, I., & Purwono, S. (2009). Understanding of mercury corrosion attack on stainless steel material at gas well: Case study. *Society of Petroleum Engineers - International Petroleum Technology Conference 2009, IPTC 2009*, *2*, 958–965.

Panagiotopoulou, P., Kondarides, D. I., & Verykios, X. E. (2009). Selective methanation of CO over supported Ru catalysts. *Applied Catalysis B: Environmental*, *88*, 470–478.

Qu, Q., Jiang, S., Li, L., Bai, W., & Zhou, J. (2008). Corrosion behavior of cold rolled steel in peracetic acid solutions. *Corrosion Science*, *50*, 35–40.

Rohtash, Singh, A. K., & Kumar, R. (2014). Corrosion study of stainless steels in peracetic acid bleach media with and without chloride and chelant. *International Journal of Research and Innovations in Science and Technology Volume*, *1*(1), 1–10.

Rosid, S. J. M., Toemen, S., Wan Abu Bakar, W. A., Zamani, A. H., & Wan Mokhtar, W. N. A. (2019). Physicochemical characteristic of neodymium oxide-based catalyst for in-situ CO 2 /H 2 methanation reaction. *Journal of Saudi Chemical Society*, *23*, 284–293.

Siddiqui, R. A., Abdul-Wahab, S. A., Pervez, T., & Qamar, S. Z. (2007). Hydrogen embrittlement in low carbon steel. *Archives of Materials Science*, *28*(1–4), 136–142.

Toemen, S., Abu Bakar, W. A. W., & Ali, R. (2016). Effect of ceria and strontia over $Ru/Mn/Al_2O_3$ catalyst: Catalytic methanation, physicochemical and mechanistic studies. *Journal of CO_2 Utilization*, *13*, 38–49.

Tong, L., Yue, T., Zuo, P., Zhang, X., Wang, C., Gao, J., & Wang, K. (2017). Effect of characteristics of KI-impregnated activated carbon and flue gas components on Hg0 removal. *Fuel*, *197*, 1–7.

Wigfield, D. C., & Perkins, S. L. (1985). Oxidation of elemental mercury by hydroperoxides in aqueous solution. *Canadian Journal of Chemistry*, *63*, 275–277.

Zhang, H., Wang, T., Liu, J., Zhang, Y., Wang, J., Sun, B., & Pan, W. P. (2020). Promotional effect of sulfur trioxide (SO3) on elemental mercury removal over Cu/ZSM-5 catalyst. *Applied Surface Science*, *511*, 145604.

Zhao, B., Yi, H., Tang, X., Li, Q., Liu, D., & Gao, F. (2019). Using CuO-MnOx/AC-H as catalyst for simultaneous removal of Hg° and NO from coal-fired flue gas. *Journal of Hazardous Materials*, *364*(December 2017), 700–709.

Zhao, Y., Hao, R., & Guo, Q. (2014). A novel pre-oxidation method for elemental mercury removal utilizing a complex vaporized absorbent. *Journal of Hazardous Materials*, *280*, 118–126.

Zhuang, Y., Laumb, J., Liggett, R., Holmes, M., & Pavlish, J. (2007). Impacts of acid gases on mercury oxidation across SCR catalyst. *Fuel Processing Technology*, *88*, 929–934.